Heterogeneity of acetylcholine receptor autoantibody-mediated complement activity in patients with myasthenia gravis.

Abeer H. Obaid[1,2,3], Chryssa Zografou[1,2], Douangsone D. Vadysirisack[4], Bailey Munro-Sheldon[1], Miriam L. Fichtner[1,2], William M. Philbrick[2], Jeffrey L. Bennett[5], Richard J. Nowak[1], and Kevin C. O'Connor[1,2]

1. Department of Neurology, Yale School of Medicine, New Haven, CT 06511 USA.
2. Department of Immunobiology, Yale School of Medicine, New Haven, CT 06511 USA.
3. Institute of Biomedical Studies, Baylor University, Waco, TX 76706 USA.
4. UCB Pharma, Cambridge, MA 02140, USA
5. Departments of Neurology and Ophthalmology, Programs in Neuroscience and Immunology, University of Colorado Anschutz Medical Campus, Aurora, Colorado, 80045, USA.

Supplemental Data: eTable 1, eTable 2, eFigure 1, eFigure 2

Search Terms: [132] Autoimmune diseases, [179] Myasthenia, Complement, Autoantibodies.

Submission Type: Article
Title Character Count (with spaces): 117
Number of Tables: 0
Number of Figures: 5
Word Count of Abstract: 327
Word Count of Paper: 4722
Number of References: 48

Corresponding Author:
Kevin C. O'Connor, PhD
Yale School of Medicine
300 George Street Room 353J
New Haven, CT 06511
Ph: 203-737-3321; *email*: kevin.oconnor@yale.edu

Study funding: KCO was supported by the National Institute of Allergy and Infectious Diseases of the NIH under award numbers R01-AI114780 and R21 AI164590; through an MGNet pilot grant awarded through the Rare Diseases Clinical Research Consortia of the NIH (award number U54-NS115054) and by a High Impact Clinical Research and Scientific Pilot Project award from the Myasthenia Gravis Foundation of American (MGFA). This project was supported, in part, by grants to KCO and RJN, from Ra Pharmaceuticals, now a part of UCB. JLB was supported by the National Eye Institute R01-EY022936 and R21-032399. MLF was supported in part by the SPIN award through Grifols and has further been supported by a DFG Research fellowship (FI 2471/1-1)

Financial disclosures:

Abeer H. Obaid reports no disclosures.

Dr. Chryssa Zografou reports no disclosures.

Dr. Douangsone D. Vadysirisack is an employee of UCB Ra Pharma.

Dr. Bailey Munro-Sheldon reports no disclosures.

Dr. Miriam L. Fichtner reports no disclosures.

Dr. William M. Philbrick reports no disclosures.

Dr. Jeffrey L. Bennett reports payment consultation fees for study design/consultation from Viela Bio, now part of Horizon Therapeutics; and personal fees from Mitsubishi Tanabe Pharma Corporation; Reistone Bio, AbbVie, Alexion; Chugai, Clene Nanomedicine, Genentech, Genzyme, Mitsubishi-Tanabe, and Roche; grants from Novartis, Mallinckrodt; and has a patent for Aquaporumab issued.

Dr. Richard J. Nowak has received research support from the National Institutes of Health (NIH), Genentech, Alexion Pharmaceuticals, argenx, Annexon Biosciences, UCB Ra Pharmaceuticals, Myasthenia Gravis Foundation of America, Momenta, Immunovant, Grifols, and Viela Bio, now part of Horizon Therapeutics. RJN has served as consultant/advisor for Alexion Pharmaceuticals, argenx, Cabaletta Bio, CSL Behring, Grifols, Ra Pharmaceuticals, now a part of UCB Pharma, Immunovant, Momenta, and Viela Bio, now part of Horizon Therapeutics.

Dr. Kevin C. O'Connor has received research support from Ra Pharma, now a part of UCB Pharma, and Alexion, now part of AstraZeneca, and Viela Bio, now part of Horizon Therapeutics. KCO is a consultant and equity shareholder of Cabaletta Bio, and is the recipient of a sponsored research subaward from the University of Pennsylvania, the primary financial sponsor of which is Cabaletta Bio. KCO has served as consultant/advisor for Alexion Pharmaceuticals, now part of AstraZeneca, and for Roche, and he has received speaking fees from Alexion, Roche, Genentech, and Viela Bio, now part of Horizon Therapeutics.

Statistical Analysis:
Statistical analyses were conducted by Abeer H. Obaid (Yale School of Medicine, Department of Neurology).

Abstract

Background Autoantibodies targeting the acetylcholine receptor (AChR) in the serum of myasthenia gravis (MG) patients are broadly polyclonal and heterogeneous in their pathogenic capacity. Specifically, AChR autoantibody-mediated pathology occurs through three mechanisms that include complement-directed tissue damage, blocking of the acetylcholine binding site on the AChR, and modulation (internalization) of the AChR. Clinical assays used for diagnosis and prognosis measure only AChR autoantibody binding and they provide weak association with disease burden, thereby limiting understanding of mechanistic heterogeneity, and monitoring therapeutic response. **Objective** To develop an *in-vitro* cell-based assay that measures AChR autoantibody-mediated complement membrane attack complex (MAC) formation. **Methods** A HEK293T cell line, which is commonly used for live cell-based AChR autoantibody binding assays, was modified such that the expression of the complement regulator genes (CD46, CD55 and CD59) were disrupted using CRISPR/Cas9 genome editing. This modified cell line was used to measure serum AChR autoantibody-mediated complement MAC formation via flow cytometry. **Results** AChR autoantibody-mediated MAC formation required the use of a modified HEK293T cell line in which the surface expression of three complement regulator genes was absent. Serum samples (n=155) from 97 clinically confirmed AChR patients were tested along with 32 healthy donor (HD) samples; the MG cohort included a wide range of disease burden and AChR autoantibody titer. AChR autoantibodies were detected in 139 of the 155 (89.7%) AChR patient samples via a live cell-based assay. Of the 139 AChR positive samples, autoantibody-mediated MAC formation was detected in 83 (59.7%), while no autoantibodies or MAC formation was detected in samples from the HD group. Autoantibody-mediated MAC formation positively associated with autoantibody binding in most MG patient samples. However, a subset displayed a disassociation between binding and MAC formation. **Conclusions** We demonstrate the development of a novel assay for evaluating AChR autoantibody-mediated complement activity. It is anticipated that this assay will afford a deeper understanding of the

heterogeneous disease pathology and allow for the identification of MG patients who may benefit from complement inhibitor therapy.

Introduction

Myasthenia gravis (MG) is an autoimmune disorder affecting neuromuscular transmission. Patients suffer from muscle weakness and increased muscle fatigability due to diminished neuromuscular signaling[1-3]. The impairment in autoimmune MG is caused by autoantibodies that target components of the neuromuscular junction (NMJ)[1, 2, 4]. The most common subtype of autoantibody-mediated MG is characterized by pathogenic autoantibodies targeting the nicotinic acetylcholine receptor (AChR)[2]. Detection of AChR autoantibodies confirms a diagnosis of MG, however titers (serum concentration) vary widely among patients and within individuals during the course of their disease, and it is generally recognized that titer does not correlate well with disease severity[5-8].

AChR autoantibodies in the serum of MG patients are broadly polyclonal and heterogeneous in their specificity, as MG serum includes autoantibodies that can recognize any of the four different AChR subunits (α, β, ε/γ, or δ)[9]. AChR autoantibodies can use three distinct mechanisms[4, 10-19] to effect pathology: (i) complement-directed tissue damage, (ii) blocking the binding site for acetylcholine on the receptor and, (iii) modulation (internalization) of the AChR. Furthermore, given the discordance between disease severity and titer, there may also be a subgroup of binding-only antibodies that recognize AChR in clinical assays but do not have any pathogenic properties.

In addition to the lack of understanding concerning the disconnect between autoantibody titer and disease severity, gaps in our knowledge have recently become more consequential because new therapeutics specifically targeting the pathogenic mechanisms of AChR autoantibodies—including complement inhibitors—have been introduced[20]. Eculizumab is a recently approved biological therapeutic for the treatment of generalized AChR MG[21]; it inhibits autoantibody-mediated activity of the terminal

complement cascade. Currently, there are no predictors of response to eculizumab therapy in MG. The phase III clinical trial showed efficacy, but approximately 40% of AChR autoantibody-positive patients did not meet the trial endpoint, without longer-term treatment, and some experienced exacerbation events requiring rescue therapy[21-23]. These data are challenging to reconcile as the poor responders had measurable circulating AChR autoantibodies. These clinical studies emphasize the limitations of AChR autoantibody titer as a biomarker, and importantly underscore the need for further understanding of AChR autoantibody-mediated pathogenic mechanisms so that response to treatments can be better predicted. To that end, we sought to develop an *in vitro* assay that measures serum-derived AChR autoantibody-mediated complement activation through measuring membrane attack complex (MAC) formation.

Methods

MG patients and serum samples

This study was approved by Yale University's Institutional Review Board (clinicaltrials.gov || NCT03792659). Informed written consent was received from all participating patients prior to inclusion in this study. Serum was collected from AChR MG patients at the Yale Myasthenia Gravis Clinic, New Haven, Connecticut, USA[24]. Detailed demographics and clinical data for the study cohort are presented in **Table e1.**

CRISPR/Cas9 genome editing of HEK293T cells

CD46, CD55 and CD59 CRISPR sgRNAs **(Table e2)** were cloned into pSpCas9(BB) -2A-Puro (PX459) vector and were transfected into HEK293T cells (ATCC CRL3216) with lipofectamine 2000 (Thermo Fisher Scientific, cat# 11668027) according to manufacturer's instructions in growth media without antibiotics. The pSpCas9(BB)-2A-Puro (PX459) V2.0 [25] was a gift from Feng Zhang (Addgene plasmid # 62988). The cells were harvested after 48 hours, and single cell dilutions were used to derive single cell clonal cell lines. These clones were then tested phenotypically for the deletion of CD46, CD55 and CD59 via PCR, Sanger sequencing, and flow cytometry. Clones that exibited CRISPR deletions underwent

FACS sorting to ensure the selection of cells with the three genes deletions. Cultures were not used beyond 10 passages and the absence of surface expression of CD46/55/59 was tested frequently via FACS.

Autoantibody binding live cell-based assay (CBA)

Wild type (WT) and triple KO HEK293T were transfected with adult AChR (2α, β, δ, and ε) and rapsyn-GFP plasmids (generous gifts from Drs. Angela Vincent, David Beeson and Patrick Waters) using branched polyethylenimine (Sigma Aldrich, Cat# 408727). After a 24-hour incubation period, the media was refreshed, and the cell-based assay was conducted the following day. Cells were exposed to serum from healthy donors (HD) or MG patients at 1:20 dilution, or monoclonal antibodies (mAbs) at a concentration of 10 μg/ml. Antibodies that bound to the AChR transfected cells were detected with an anti-human IgG Fcγ (309-605-008; Jackson ImmunoResearch). Cells were run on a BD LSR Fortessa (BD Biosciences) at the Yale School of Medicine, Laboratory Medicine Immune Monitoring Core Facility. FlowJo software (v10.6.2) was used to conduct the analysis. In serial dilution testing, some serum samples can provide aberrantly low CBA ΔMFI values when tested at 1:20, due to assay saturation and/or interference; accordingly, these data points were not considered in the analyses. For testing AQP4 binding, HEK293T cells were transiently transfected with vector encoding AQP4-GFP (M1 isoform) as previously described[26], using the same CBA conditions described for AChR testing.

Chinese Hamster Ovary (CHO) cells (CCL-61) were either transfected using branched polyethylenimine or with Lipofectamine 2000 following the manufacturer's instructions for the latter. To test for approaches to reduce background binding, CHO cells were blocked with 10% goat sera for 1 hour at 4 °C or the heat-inactivated sera was pre-cleared of CHO-reactive antibodies by incubating with untransfected CHO cells for 1 hour at 4 °C. Other aspects of the CHO CBA were conducted as described for the HEK293T cells (above).

Complement reagents and antibodies

Commercial complement competent normal human serum and factor B-depleted human serum were both purchased from Complement Technologies (Tyler, TX). Primary antibodies for flow cytometry analysis include CD46 clone TRA-2-10 (Cat# 352403), CD55 clone JS11 (Cat# 311301), CD59 clone H19 (Cat# 304701) and secondary antibodies PE Cy7 IgG1 clone RMG1-1 (Cat# 406613) and APC (Cat # 407109) or PE IgG2a clone RMG2a-62 (Cat# 407109), and were all purchased from Biolegend. MAC formation was measured using commercially available anti-C9 neoantigen (Hycult, Cat# HM2264).

Complement cell-based assay (CCBA)

CD46, CD55, CD59 KO HEK293T cells or CHO cells were prepared as outlined in the live cell-based assay. Cells were washed twice and resuspended in complete DMEM. Cells were exposed to AChR MG patient serum (heat-inactivated), HD serum (heat-inactivated), or control mAb suspended in 25% normal human serum (NHS) (Complement Technologies) or Factor B depleted serum (Complement Technologies). MAC formation was allowed to proceed for 3 hours at 37°C with rocking, after which the cells were washed twice with FACS buffer (1% BSA PBS) and fixed with 2% PFA at 4°C for 15 minutes. The cells were then washed twice with FACS buffer, and then stained with anti-C9 neoantigen (Hycult, Cat# HM2264), followed by washing and secondary staining (APC IgG2a). Cells were run on BD LSR Fortessa (BD Biosciences) at the Yale School of Medicine, Laboratory Medicine Immune Monitoring Core Facility. FlowJo software (v10.6.2) was used to conduct the analysis.

Expression of human recombinant monoclonal antibodies

Human recombinant mAbs were expressed as we have previously described[27]. In short, HEK293A cells were transfected with 3μg each of human antibody heavy and light chain plasmids using linear polyethylenimine (Polysciences, Cat #23966). After a 24-hour incubation, the transfection media was

substituted for basal media (50% DMEM 12430, 50% RPMI 1640, 1% antibiotic/antimycotic, 1% Na-pyruvate (Thermo Fisher Scientific) and 1% Nutridoma (Sigma Aldrich, Cat# 11011375001)). Expression proceeded for 6 days, after which the supernatant was collected. The recombinant mAbs were then purified from the supernatant with protein G Sepharose 4 Fast Flow beads using the manufacturer's recommend purification protocol (GE Healthcare Life Sciences).

Statistics

Thresholds for positivity for the CBA and complement CBA were determined by the application of a cutoff value. The values were determined by calculating the mean plus 4 standard deviations of HD subject samples. MAC formation comparison between HD and MG samples was analyzed using nonparametric Mann-Whitney U test. The relationship between CBA and MAC formation was evaluated with a non-parametric Spearman correlation. P-values below 0.05 were considered significant. All statistical analyses were performed on Graphpad Prism software (v9.1.2).

Results

Measuring autoantibody-mediated MAC formation using a cell-based assay platform

Live cell-based assays (CBA) are frequently used to measure AChR autoantibodies[28, 29]. In this assay format, recombinant human AChR subunits are expressed in human embryonic kidney (HEK) cells and tested for binding of antibodies by flow cytometry. Co-transfection with the clustering protein, rapsyn increases sensitivity[30]. We sought to measure AChR autoantibody-mediated complement activity by modifying the clustered AChR CBA platform. To that end, the assay was performed by using autoantibodies (recombinant mAbs or autoimmune patient-derived serum, in which the complement was heat-inactivated) and normal human serum (NHS) as a consistent complement source, and testing antibody-dependent MAC formation by measuring the presence of a C9 neo-epitope revealed following MAC formation with flow cytometry. We first evaluated antibody-dependent MAC formation with the

modified CBA using an established positive control; specifically, human aquaporin (AQP4) autoantibodies from patients with neuromyelitis optica spectrum disorder (NMOSD), which have been demonstrated to efficiently fix complement *in vitro*[31]. AQP4 was expressed in HEK293T cells, then a human AQP4-specific recombinant IgG1 subclass mAb (mAb-58[32]) was added (10 μg/mL) along with NHS. MAC formation was detected when AQP4-specific mAb and NHS were present but was not detected in the absence of either the AQP4-specific mAb or NHS **(Figure 1A)**. In addition, the MAC was not detected when the AQP4-specific mAb was tested with NHS in which the complement proteins were heat-inactivated. Serum (1:20 dilution) from an AQP4 autoantibody positive NMOSD patient also mediated MAC formation when tested with NHS, but not without NHS or when heat-inactivated NHS was present **(Figure 1B)**. Serum from a healthy control (HD-29), which was tested under the same conditions, did not initiate MAC formation **(Figure 1B)**. Having demonstrated that the CBA could detect autoantibody-dependent MAC formation, we next tested AChR autoantibody-mediated MAC deposition under the same conditions used for testing the AQP4 autoantibodies. An AChR-specific human recombinant IgG1 subclass mAb (mAb-637, 10μg/mL)[33] and an AChR autoantibody positive MG serum sample (MG-87 tested at 1:20), were tested with the complement CBA using AChR-rapsyn expression. In contrast to the results obtained in the AQP4 system, no AChR-autoantibody-dependent MAC deposition was detected with the mAb or the MG serum **(Figure 1C)**.

AChR cell-based assay and CHO cells

Most human cells contain complement regulators on their cell surface, namely CD46, CD55 and CD59 that can interfere with complement deposition. Therefore, we tested the CBA with CHO cells, as these non-human cells do not endogenously express these factors on their cell surface[34]. First, we investigated whether CHO cells can be transfected with PEI and found the efficiency to be low **(eFigure 1A)**. We were able to increase the efficiency by approximately 20-fold by using lipofectamine **(eFigure 1A)**. Here, mAb-637 could be detected on AChR-transfected CHO cells over a broad range of concentrations, while

rapsyn-only transfected cells showed no binding signal **(eFigure 1B).** Next, we investigated whether CHO cells can be used for the complement (MAC) deposition assay **(eFigure 1C)**. However, there was high non-specific background binding associated with the NHS; we speculated that non-specific binding of human IgG from either the NHS or the heat-inactivated sera might be responsible for this observation. Thus, we tested HD samples on rapsyn-only transfected cells for nonspecific binding **(eFigure 1D)**. To further reduce nonspecific binding, the CHO cells were blocked with goat serum and the sera was pre-cleared by incubation with the CHO cells. Neither blocking nor preclearing or a combination of both had any effect on reducing the nonspecific background binding. In summary, we were able to establish an AChR-specific cell-based binding assay with CHO cells, but nonspecific background binding by human IgG prevented its use for complement detection.

Disrupting expression of complement regulators in HEK293T cells

A previous study demonstrated that the human HAP1 cell line, in which the expression of several complement regulators was disrupted through gene editing, provided increased complement component deposition upon activation of the classical pathway[35]. Thus, we reasoned that a genome edited HEK293T cell line in which the complement regulators CD46, CD55 and CD59 were not expressed, would be an effective tool in evaluating AChR autoantibody-mediated complement activity. To produce a modified HEK293T cell line, CRISPR/Cas9 genome editing was used to target these genes in HEK293T cells **(Figure 2A, eTable 2).** Several single cell clones underwent multiple rounds of CRISPR editing and were then sorted for triple negative populations **(Figure 2B).** Of these clones, protein expression on the cell surface was assessed via FACS analysis, and no expression of CD46, CD55 and CD59 was observed compared to WT HEK293T cells **(Figure 2C).**

Autoantibody binding live cell-based assay in the absence of complement regulators

To confirm that AChR binding by the autoantibodies was not compromised in the modified HEK293T cells, the CD46/55/59 KO cells were compared with WT HEK239T cells in a live CBA. Both cell types

were transiently transfected with AChR, after which the cells were exposed to either AChR-specific human recombinant mAb-637 (10 μg/mL), MG or HD serum (diluted 1:20). WT HEK and triple KO cells showed indistinguishable antibody binding patterns with mAb-637 and MG serum. No autoantibody binding with HD serum was observed in either cell lines **(eFigure 2)**.

AChR autoantibody-mediated MAC formation in the absence of complement regulators

The CD46/55/59 KO HEK293T engineered cells were then tested in the complement CBA, first using the AQP4 antigen. AQP4 was expressed through transient transfection, then the AQP4-specific mA-58 (10 μg/mL) or heat-inactivated serum (1:20) from AQP4 autoantibody positive NMOSD patient, was added to the cells and tested for MAC formation as described for the WT HEK cells. MAC formation was detected when the AQP4-specific mAb (10 μg/mL) or serum from an AQP4 autoantibody positive NMOSD patient were added together with NHS. Conversely, MAC formation was not detected in the absence of either the AQP4 autoantibody source or NHS, or when the mAb or serum was added with heat-inactivated NHS **(Figure 3A)**. The AChR-specific mAb-637, serum from a patient with MG and healthy controls, which were tested under the same conditions, did not initiate MAC formation in the AQP4 complement CBA **(Figure 3A)**. To test the complement CBA with the modified cells for AChR autoantibody-mediated MAC formation, AChR and rapsyn were co-expressed, then the 637-mAb (10 μg/mL) was added to the cells and tested for MAC formation. MAC formation was detected when the AChR-specific mAb and NHS were present but not in the absence of either the AChR mAb or NHS, or when the mAb was added with heat-inactivated NHS **(Figure 3B)**. We next tested MAC formation with serum samples from four AChR autoantibody positive MG patients and four non-MG serum samples. Two were derived from MG patients **(eTable 1)** with AChR autoantibody titers—as measured by the clinical diagnostic radioimmunoassay (RIA)—that were exceptionally high (MG-87 and MG-56, 43nM and 88nM respectively) and two with mid-low range titers (MG-43 and MG-44, 14.3nM and 1.47nM respectively). Serum from one of the four MG patients mediated robust MAC formation **(Figure 3C)**

when added with NHS. Interestingly, MG-87 did not mediate MAC formation in the complement CBA, when using the WT HEK293T cells **(Figure 1C)**. MAC formation was not observed with MG-87 in the absence of NHS or when heat-inactivated NHS was present **(Figure 3C)**. Serum from two of the four MG patients mediated weak MAC formation and the remaining sample showed none. The non-MG controls, which included HD serum samples, NMOSD serum, and AQP4-specific mAb-58, did not mediate MAC formation on the AChR-expressing cells when tested under the same conditions **(Figure 3C)**.

To confirm that the antibody-mediated classical complement pathway was generating the MAC, we tested whether the alternative pathway was contributing to the MAC formation. This was achieved through inhibiting the alternative pathway by using NHS in which factor B, which is required for the alternative pathway, was depleted. AQP4 was expressed, then the AQP4-specific mAb-58 (10 μg/mL) was added to the cells and tested for MAC formation using factor B depleted serum in place of NHS as the complement source. The MAC was detected when mAb-58 and factor B depleted serum were present but not in the absence of either the AQP4 autoantibody or factor B depleted serum, or when the mAb was added with heat-inactivated factor B depleted serum **(Figure 3D)**. Finally, to confirm that the self-antigen was driving autoantibody binding and subsequent MAC formation, non-transfected cells were tested in the complement CBA using the AQP4-specific mAb-58, AChR-specific mAb-637, HD serum, and an MG patient serum sample (MG-87), which demonstrated MAC deposition with the AChR transfected cells. No MAC formation was observed with these mAbs and serum sample when their respective antigen was not expressed on the modified HEK cells **(Figure 3E)**.

Testing MG patient serum for autoantibody-mediated MAC formation.

Having demonstrated that the complement CBA could measure AChR autoantibody-mediated classical pathway MAC formation, we next tested MG serum samples to explore how AChR autoantibody-mediated complement activity was represented in a heterogeneous population of MG patients. MAC deposition was tested using heat inactivated serum from 30 HD subjects (n=32 samples) and from 97

patients (n=155 samples) with a confirmed diagnosis of AChR MG (**eTable 1**). While all the MG patients were diagnosed with the AChR disease subtype, we specifically included patient samples that were AChR autoantibody positive and others that were negative at the time of collection (**eTable 1**). An assay positivity cut-off was established using the mean MAC mean florescence intensity (MFI) from the HD cohort (156±14); samples with an MFI > mean + 4SD of the HD cohort were considered positive. Serum from the HD cohort did not show any measurable AChR autoantibody-mediated MAC deposition **(Figure 4A)**. A subset (83/155, 59.7 %) of the MG patient-derived samples, demonstrated AChR autoantibody-mediated MAC deposition **(Figure 4A)**. To determine whether those samples, which did not mediate MAC formation, included autoantibodies that were detectable by CBA, we next evaluated the association between MAC deposition and AChR autoantibody binding by comparing the complement CBA results to those of the antibody binding CBA. There was a significant correlation ($r=0.897$; $p<0.0001$) observed between MAC deposition and AChR binding **(Figure 4B)**. Samples for which there was no detectable binding in the CBA did not mediate detectable MAC formation in the complement CBA. Additionally, samples that provided a positive, yet low, signal in the binding CBA did not mediate detectable MAC formation.

We observed subsets of samples within the cohort that showed a disproportionate association between MAC deposition and AChR binding. Specifically, several samples provided a low signal in the MAC deposition CBA (<500 MFI) but a strong signal (>750 ΔMFI) in the AChR binding CBA **(Figure 4B)**. Additionally, there was a subset of samples that showed a different association: strong CBA binding signals (>750 ΔMFI) with exceptionally high (>1300 MFI) MAC deposition signals, which were considerably higher than other samples with similar binding CBA signals. These collective results suggest that, for the majority of MG patient serum AChR autoantibodies, CBA binding positively associates with autoantibody-mediated CBA MAC deposition.

Comparing titers of MG patient serum autoantibody binding and autoantibody-mediated MAC formation

While CBA-based binding and MAC formation were closely associated for many samples, the results also suggest that a subset of patients may harbor AChR binding autoantibodies that range broadly in their ability to mediate MAC formation. To further explore the dissociation observed between MAC formation and AChR binding, 14 samples were selected for further study **(Figure 4B),** based on their observed incongruence between the MAC formation and AChR binding. Each sample was tested for AChR autoantibody binding and MAC formation at various serum dilutions **(Figure 5)**. The binding CBA, which tested serum over three-fold dilutions from 1:20-1:1350, showed a range of binding titers. The complement CBA, which tested serum over two-fold dilutions from 1:20-1:320, showed a wide range of MAC formation. Of interest was that several samples showed similarly strong AChR binding profiles but differed considerably in their MAC formation capability **(Figure 5)**. For example, samples MG-20 and MG-34 have comparable binding profiles but considerably differ in their MAC formation capability; MG-20 mediated robust MAC formation at three of the serum dilutions tested, while MG-34 did not provide a signal above the cut-off at any serum dilution. Similarly, MG-49, MG-51 and MG-89 provided strong binding signals, but only MG-89 provided a strong MAC formation signal. These collective results imply that the autoantibodies harbored by these patients have differing pathogenic capacities irrespective of binding capability.

Discussion

We have established an assay that quantitatively assesses serum-derived AChR autoantibody-mediated MAC deposition. The assay is founded on a live cell-based assay (CBA) in which clustered AChR is expressed for high sensitivity measurements of autoantibody binding[30]. A modification of the binding assay, in which the expression of complement regulators was interrupted, was required for AChR autoantibody-mediated MAC deposition. Comparing a clinically heterogeneous set of MG patients revealed differences in autoantibody-mediated MAC formation that was not consistently associated with binding to the autoantigen. Thus, these findings demonstrate the development of an assay for evaluating

AChR autoantibody-mediated MAC formation and that this activity can be heterogeneous given the variable molecular properties and characteristics of circulating AChR autoantibodies.

The heterogeneity of AChR autoantibody-mediated pathology

Detection of AChR autoantibodies confirms a diagnosis of MG, however titers vary widely between different patients and within individuals during their disease progression. Although AChR autoantibodies directly contribute to pathogenesis, it is generally recognized that their serum concentration (titer), when measured by RIA in commercial clinical laboratories, does not correlate well with disease severity among different patients[5-8]. The discordance between titer and disease severity may be, in part, due to how AChR autoantibody titer is measured. Specifically, the clinical assays used to diagnose patients and provide titer values are unable to discriminate between the detection of the autoantibodies and their pathogenic properties (effector functions). AChR MG autoantibodies are thought to mediate their pathogenic capacity through three specific mechanisms: (i) complement-directed tissue damage, (ii) blocking the attachment of acetylcholine (ACh) by binding directly to the site on the AChR that recognizes ACh and (iii) modulation (internalization) of the AChR through crosslinking of the receptor[4, 10-19]. Importantly, nonpathogenic binding-only autoantibodies, which would be detected in clinical assays, may also exist, further complicating the disconnect between disease severity and autoantibody titer.

Our data revealed a positive association between autoantibody binding and MAC formation, suggesting that a considerable fraction of circulating AChR autoantibodies can initiate the complement cascade. However, binding alone did not account for the variation observed in complement activity. We reason that heterogeneous characteristics of the autoantibodies, among other factors, may play an integral role in determining MAC formation efficiency. Such autoantibody characteristics would minimally include subunit and epitope specificity, affinity, IgG subclass usage, and post-translation modifications (PTM), all of which can alter complement activating capability in addition to structure and stability[36, 37]. Although it is currently unclear how AChR autoantibody heterogeneity affects MAC formation in MG patients,

parallels to the mechanisms governing AQP4 autoantibody-mediated pathology in NMOSD provide insight. AQP4-binding autoantibodies display broad efficiency in inducing complement-mediated cell death[31]. Here, a combination of distinct properties, including particular epitope binding and the assembly of multimeric antigen platforms, are required for ideal activation of autoantibody complement-mediated cell death[31]. Specifically, AQP4 autoantibodies that target a distinct epitope on the extracellular loop C of AQP4 demonstrate remarkably enhanced complement activity when compared to autoantibodies recognizing other epitopes on AQP4. Furthermore, AQP4 can form supramolecular orthogonal arrays that arrange these epitopes in a manner that benefits autoantibody multimeric complexes supporting autoantibody Fc-Fc interactions, which are critical for efficient C1q binding and subsequent complement activity[31]. Whether or not similar mechanisms occur in the context of AChR-specific MG has yet to be explored. However, given the variable complement activity shown here and that AChR is tightly clustered by the intracellular scaffolding protein, rapsyn, such organized formations of self-antigen may support Fc-Fc interactions facilitating efficient complement activation, by AChR autoantibodies recognizing particular—but not yet identified—epitopes. Thus, we propose that circulating AChR autoantibodies include subtypes comprising heterogeneous pathogenetic mechanisms and variable efficiency in affecting these mechanisms, and finally that their composition varies among patients, and perhaps longitudinally within a patient. We further suggest that AChR autoantibody subunit specificity and epitope specificity is linked to these effector functions, including activation of the classical complement pathway.

Study limitations

We recognize that this study includes limitations. First, the HEK293T is a hypotriploid human cell line that exhibits a 64 modal chromosome number. This complexity created a significant challenge for the generation of the complement regulator knockout compared to other cells lines such as HAP1 which are haploid. We frequently monitored the absence of surface expression of CD46, CD55 or CD59 and continued to use the cell line at early passages (<10) to avoid the development of a heterogeneous culture. Further genetic engineering and analysis will be required to generate a stable single cell-derived clone. To

avoid the challenges presented by knocking out three genes in a hypotriploid human cell line, we also evaluated the use of Chinese hamster ovary cells (CHO) for the CBA, given their lack of CD46, CD55 or CD59 expression. However, the use of a nonhuman cell line generated unacceptably high non-specific background binding with human serum samples. Second, measuring complement formation on live cells with flow cytometry presents challenges given that the cells are actively dying and lysing and therefore are not recognized by the instrument. We empirically arrived at a single timepoint after the addition of NHS that provided measurable differences in MAC deposition in the AQP4 and AChR complement CBAs when comparing patient samples and controls. This approach was chosen in consideration of assay ease-of-use. Longitudinal measurements after the addition of NHS or different approaches that measure cumulative cell death, such as Cr^{52} release, may provide additional information on AChR autoantibody-mediated activity, but was outside the scope of our study. Finally, we recognize that the *in vitro* autoantibody-mediated complement activity may not fully reflect an *in vivo* complement response. We are using an *in vitro* system with diminished expression of complement inhibitory proteins. Our system reflects the capability of the autoantibody to initiate complement but does not consider the varying levels of complement inhibitory protein expression on various muscle cell surfaces. For example, CD55 knockout mice have been shown to be more susceptible to the effects of pathogenic MG autoantibodies[38-40]. The expression of these inhibitors has also been implicated in ocular MG, where reduced expression levels of CD55 and CD59 in extraocular muscles offer a potential explanation for why these muscle subgroups are highly associated with MG[38].

Clinical utility of measuring AChR autoantibody mediated pathogenesis

The last decade has seen a considerable number of new and existing therapeutics become available for the treatment of MG[20]. The majority include biologics that target the autoantibodies or the B cells that produce them. Specific examples include B cell depletion mediated through anti-CD20 (rituximab)[41, 42] or anti-CD19 (inebilizumab)[43]; suppressing B cell activity by targeting BLyS (belimumab)[44]; inhibiting complement activation (eculizumab and others)[45]; and reducing IgG levels by inhibiting FcRn

(efgartigimod and others)[46]. Clinical trials of these treatments have provided outcomes demonstrating benefit in some MG patients but unexpected failure in other patients. The outcomes from these trials have also intensified challenges to the field. Specific challenges include the need to target the correct therapy to patients from the growing number of options, and the need to inform treatment decisions through understanding the immunopathology. Therapeutic strategies that specifically target AChR autoantibodies also provide findings that seem disconnected from titer and demonstrate the lack of a full understanding of AChR MG immunomechanisms. For instance, it is unclear why complement inhibitory therapeutic eculizumab (ECU) (approved for the treatment of generalized AChR MG[21]) does not yield clinical benefit in some AChR autoantibody-positive patients[21, 22], even with longer-term treatment[23]. The AChR autoantibody titers of the patients that responded to ECU treatment did not predict treatment efficacy nor correlate with its progression. In addition to emphasizing the limitations of AChR autoantibody titer as a valuable biomarker, these studies also underscore the need for further understanding of AChR autoantibody mechanisms so that response to treatments can be better predicted. We suggest that a suite of clinical assays that measure the composition of AChR autoantibody pathogenic mechanisms will be valuable. These assays would ideally measure binding-only, classical complement activation as shown here, and modulating and blocking functions, which have been demonstrated with similar CBA platforms[47, 48]. The major advantage in studying these nuances is it will allow patients to have a more individualized treatment plan that targets their unique autoantibody-mediated pathogenic pathways.

Acknowledgements

The authors thank Drs. Soumya Yandamuri and Gianvito Masi, and Sarah Ohashi for critical reading of the manuscript and Karen Boss for providing editorial assistance.

References

1. Gilhus NE, Skeie GO, Romi F, Lazaridis K, Zisimopoulou P, Tzartos S. Myasthenia gravis - autoantibody characteristics and their implications for therapy. Nat Rev Neurol 2016;12:259-268.

2. Vincent A. Unravelling the pathogenesis of myasthenia gravis. Nat Rev Immunol 2002;2:797-804.

3. Yi JS, Guptill JT, Stathopoulos P, Nowak RJ, O'Connor KC. B cells in the pathophysiology of myasthenia gravis. Muscle Nerve 2018;57:172-184.

4. Vincent A, Beeson D, Lang B. Molecular targets for autoimmune and genetic disorders of neuromuscular transmission. Eur J Biochem 2000;267:6717-6728.

5. Vincent A, Newsom Davis J. Anti-acetylcholine receptor antibodies. J Neurol Neurosurg Psychiatry 1980;43:590-600.

6. Lefvert AK, Bergstrom K, Matell G, Osterman PO, Pirskanen R. Determination of acetylcholine receptor antibody in myasthenia gravis: clinical usefulness and pathogenetic implications. J Neurol Neurosurg Psychiatry 1978;41:394-403.

7. Lindstrom JM, Seybold ME, Lennon VA, Whittingham S, Duane DD. Antibody to acetylcholine receptor in myasthenia gravis. Prevalence, clinical correlates, and diagnostic value. Neurology 1976;26:1054-1059.

8. Tindall RS. Humoral immunity in myasthenia gravis: clinical correlations of anti-receptor antibody avidity and titer. Ann N Y Acad Sci 1981;377:316-331.

9. Tzartos SJ, Barkas T, Cung MT, et al. Anatomy of the antigenic structure of a large membrane autoantigen, the muscle-type nicotinic acetylcholine receptor. Immunol Rev 1998;163:89-120.

10. Koneczny I, Cossins J, Vincent A. The role of muscle-specific tyrosine kinase (MuSK) and mystery of MuSK myasthenia gravis. J Anat 2013.

11. Viegas S, Jacobson L, Waters P, et al. Passive and active immunization models of MuSK-Ab positive myasthenia: electrophysiological evidence for pre and postsynaptic defects. Exp Neurol 2012;234:506-512.

12. Lindstrom JM, Engel AG, Seybold ME, Lennon VA, Lambert EH. Pathological mechanisms in experimental autoimmune myasthenia gravis. II. Passive transfer of experimental autoimmune myasthenia gravis in rats with anti-acetylcholine recepotr antibodies. J Exp Med 1976;144:739-753.

13. Oda K, Korenaga S, Ito Y. Myasthenia gravis: passive transfer to mice of antibody to human and mouse acetylcholine receptor. Neurology 1981;31:282-287.

14. Sterz R, Hohlfeld R, Rajki K, et al. Effector mechanisms in myasthenia gravis: end-plate function after passive transfer of IgG, Fab, and F(ab')2 hybrid molecules. Muscle Nerve 1986;9:306-312.

15. Howard FM, Jr., Lennon VA, Finley J, Matsumoto J, Elveback LR. Clinical correlations of antibodies that bind, block, or modulate human acetylcholine receptors in myasthenia gravis. Ann N Y Acad Sci 1987;505:526-538.

16. Drachman DB, Angus CW, Adams RN, Michelson JD, Hoffman GJ. Myasthenic antibodies cross-link acetylcholine receptors to accelerate degradation. N Engl J Med 1978;298:1116-1122.

17. Drachman DB, Adams RN, Josifek LF, Self SG. Functional activities of autoantibodies to acetylcholine receptors and the clinical severity of myasthenia gravis. N Engl J Med 1982;307:769-775.

18. Kao I, Drachman DB. Myasthenic immunoglobulin accelerates acetylcholine receptor degradation. Science 1977;196:527-529.

19. Gomez CM, Richman DP. Anti-acetylcholine receptor antibodies directed against the alpha-bungarotoxin binding site induce a unique form of experimental myasthenia. Proc Natl Acad Sci U S A 1983;80:4089-4093.

20. Nguyen-Cao TM, Gelinas D, Griffin R, Mondou E. Myasthenia gravis: Historical achievements and the "golden age" of clinical trials. J Neurol Sci 2019;406:116428.

21. Howard JF, Jr., Utsugisawa K, Benatar M, et al. Safety and efficacy of eculizumab in anti-acetylcholine receptor antibody-positive refractory generalised myasthenia gravis (REGAIN): a phase 3, randomised, double-blind, placebo-controlled, multicentre study. Lancet Neurol 2017;16:976-986.

22. Muppidi S, Utsugisawa K, Benatar M, et al. Long-term safety and efficacy of eculizumab in generalized myasthenia gravis. Muscle Nerve 2019;60:14-24.

23. Howard JF, Jr., Karam C, Yountz M, O'Brien FL, Mozaffar T, Group RS. Long-term efficacy of eculizumab in refractory generalized myasthenia gravis: responder analyses. Ann Clin Transl Neurol 2021;8:1398-1407.

24. Anil R, Kumar A, Alaparthi S, et al. Exploring outcomes and characteristics of myasthenia gravis: Rationale, aims and design of registry - The EXPLORE-MG registry. J Neurol Sci 2020;414:116830.

25. Ran FA, Hsu PD, Wright J, Agarwala V, Scott DA, Zhang F. Genome engineering using the CRISPR-Cas9 system. Nat Protoc 2013;8:2281-2308.

26. Stathopoulos P, Chastre A, Waters P, et al. Autoantibodies against Neurologic Antigens in Nonneurologic Autoimmunity. J Immunol 2019;202:2210-2219.

27. Takata K, Stathopoulos P, Cao M, et al. Characterization of pathogenic monoclonal autoantibodies derived from muscle-specific kinase myasthenia gravis patients. JCI Insight 2019;4:e127167.

28. Vincent A, Waters P, Leite MI, et al. Antibodies identified by cell-based assays in myasthenia gravis and associated diseases. Ann N Y Acad Sci 2012;1274:92-98.

29. Rodriguez Cruz PM, Huda S, Lopez-Ruiz P, Vincent A. Use of cell-based assays in myasthenia gravis and other antibody-mediated diseases. Exp Neurol 2015;270:66-71.

30. Leite MI, Jacob S, Viegas S, et al. IgG1 antibodies to acetylcholine receptors in 'seronegative' myasthenia gravis. Brain 2008;131:1940-1952.

31. Soltys J, Liu Y, Ritchie A, et al. Membrane assembly of aquaporin-4 autoantibodies regulates classical complement activation in neuromyelitis optica. J Clin Invest 2019;130:2000-2013.

32. Bennett JL, Lam C, Kalluri SR, et al. Intrathecal pathogenic anti-aquaporin-4 antibodies in early neuromyelitis optica. Ann Neurol 2009;66:617-629.

33. Graus YF, de Baets MH, Parren PW, et al. Human anti-nicotinic acetylcholine receptor recombinant Fab fragments isolated from thymus-derived phage display libraries from myasthenia gravis

patients reflect predominant specificities in serum and block the action of pathogenic serum antibodies. J Immunol 1997;158:1919-1929.

34. Saifuddin M, Hedayati T, Atkinson JP, Holguin MH, Parker CJ, Spear GT. Human immunodeficiency virus type 1 incorporates both glycosyl phosphatidylinositol-anchored CD55 and CD59 and integral membrane CD46 at levels that protect from complement-mediated destruction. J Gen Virol 1997;78 (Pt 8):1907-1911.

35. Thielen AJF, van Baarsen IM, Jongsma ML, Zeerleder S, Spaapen RM, Wouters D. CRISPR/Cas9 generated human CD46, CD55 and CD59 knockout cell lines as a tool for complement research. J Immunol Methods 2018;456:15-22.

36. Alter G, Ottenhoff THM, Joosten SA. Antibody glycosylation in inflammation, disease and vaccination. Semin Immunol 2018;39:102-110.

37. Quast I, Keller CW, Maurer MA, et al. Sialylation of IgG Fc domain impairs complement-dependent cytotoxicity. J Clin Invest 2015;125:4160-4170.

38. Kaminski HJ, Li Z, Richmonds C, Lin F, Medof ME. Complement regulators in extraocular muscle and experimental autoimmune myasthenia gravis. Exp Neurol 2004;189:333-342.

39. Lin F, Kaminski HJ, Conti-Fine BM, Wang W, Richmonds C, Medof ME. Markedly enhanced susceptibility to experimental autoimmune myasthenia gravis in the absence of decay-accelerating factor protection. J Clin Invest 2002;110:1269-1274.

40. Kaminski HJ, Kusner LL, Richmonds C, Medof ME, Lin F. Deficiency of decay accelerating factor and CD59 leads to crisis in experimental myasthenia. Exp Neurol 2006;202:287-293.

41. Diaz-Manera J, Martinez-Hernandez E, Querol L, et al. Long-lasting treatment effect of rituximab in MuSK myasthenia. Neurology 2012;78:189-193.

42. Robeson KR, Kumar A, Keung B, et al. Durability of the Rituximab Response in Acetylcholine Receptor Autoantibody-Positive Myasthenia Gravis. JAMA Neurol 2016.

43. Cree BAC, Bennett JL, Kim HJ, et al. Inebilizumab for the treatment of neuromyelitis optica spectrum disorder (N-MOmentum): a double-blind, randomised placebo-controlled phase 2/3 trial. Lancet 2019.

44. Hewett K, Sanders DB, Grove RA, et al. Randomized study of adjunctive belimumab in participants with generalized myasthenia gravis. Neurology 2018;90:e1425-e1434.

45. Howard JF, Jr., Barohn RJ, Cutter GR, et al. A randomized, double-blind, placebo-controlled phase II study of eculizumab in patients with refractory generalized myasthenia gravis. Muscle Nerve 2013;48:76-84.

46. Howard JF, Jr., Bril V, Burns TM, et al. Randomized phase 2 study of FcRn antagonist efgartigimod in generalized myasthenia gravis. Neurology 2019;92:e2661-e2673.

47. Lozier BK, Haven TR, Astill ME, Hill HR. Detection of acetylcholine receptor modulating antibodies by flow cytometry. Am J Clin Pathol 2015;143:186-192; quiz 305.

48. Cromar A, Lozier BK, Haven TR, Hill HR. Detection of Acetylcholine Receptor Blocking Antibodies by Flow Cytometry. Am J Clin Pathol 2016;145:81-85.

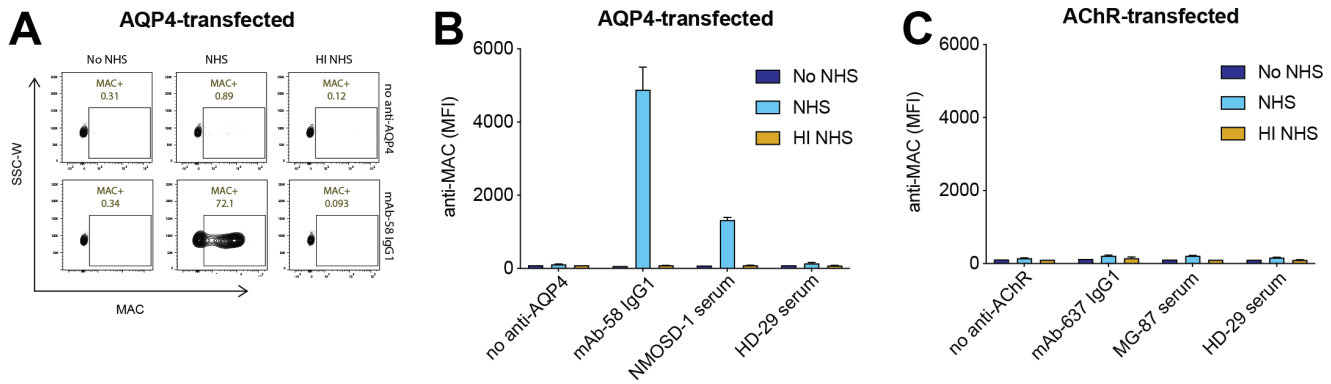

Figure 1. Autoantibody-mediated complement fixation assay using HEK293T cells. Autoantibodies were tested for their ability to mediate complement activation by measuring MAC formation on live cells transfected with self-antigens. **A.** Representative FACS plots showing MAC formation in AQP4 transfected HEK293T cells using an *in vitro* complement cell-based assay (CBA). Very low MAC assemblies were detected in the absence of a complement source (normal human serum (NHS)), or heat inactivated normal human serum (HI NHS), while MAC-positive cells were observed when a monoclonal antibody (anti-AQP4 mAb-58 IgG1) was added with normal human serum (*NHS is included as a consistent and controlled source of human complement*). *Gating strategy:* HEK293T → single cell (SSC-W vs SSC-H) → single cells (FSC-W vs FSC-H) → antigen (*measured by GFP*) positive cells. **B and C.** Measurement of MAC deposition using an *in vitro* complement CBA on AQP4 or AChR transfected cells. Cells were incubated with both the antibody and NHS for 3 hours at 37°C. Complement fixation was activated by the addition of normal human serum and anti-AChR or anti-AQP4 antibody sources (mAb-58 IgG1 (anti-AQP4 monoclonal), NMO patient serum (NMOSD-1), mAb-637 IgG1 (anti-AChR monoclonal), MG patient serum (MG-87). Controls included no addition of antibody source or healthy donor serum (HD-29). Very low MAC assemblies were detected with AChR transfected cells. Each data bar represents the mean of duplicate experimental conditions. Blank- no serum, NHS- normal human serum, HI NHS- heat inactivated normal human serum.

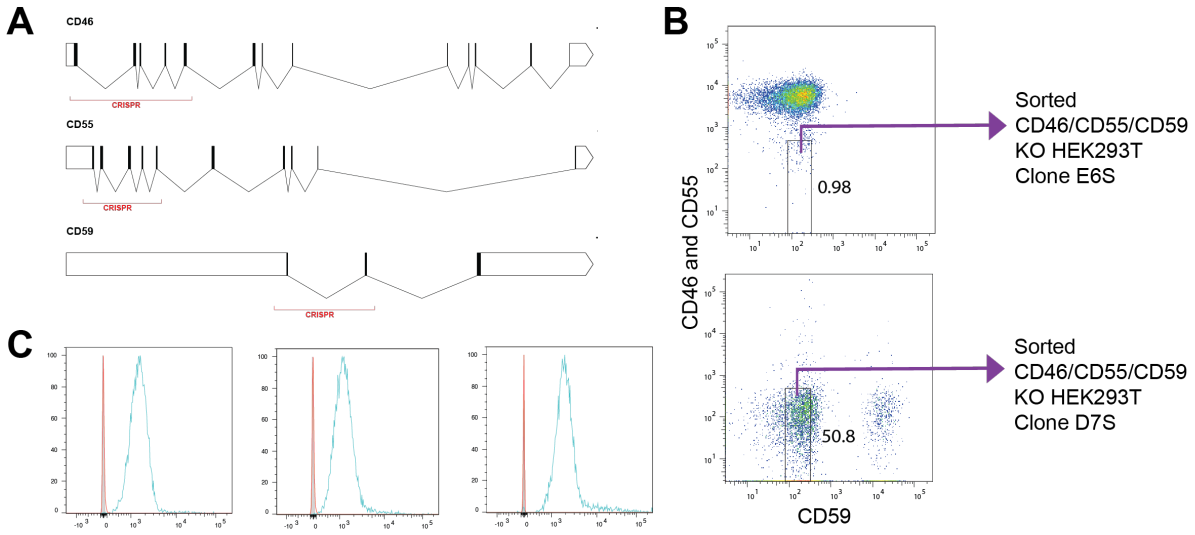

Figure 2. Design and testing of HEK293T cells engineered to lack surface expression of CD46, CD55 and CD59. A. Schematic of sgRNA primer positions for CRISPR/Cas9. **B.** FACS analysis of two single cell derived CD46/CD55/CD59 CRISPR/Cas9 genome edited HEK293T clones which were sorted for pure CD46/55/59 deficient cells. *Gating strategy:* CD46/55/59 KO HEK293T → single cell (SSC-W vs SSC-H) → single cells (FSC-W vs FSC-H) → CD59/CD55/CD46 negative population sorted **C**. FACS analysis of CD46, CD55 and CD59 expression on WT (blue) and CD46/55/59 KO HEK293T cell (red). No expression of the genes was observed on the KO line as indicated by its peak overlapping with the unstained and secondary only control (grey).

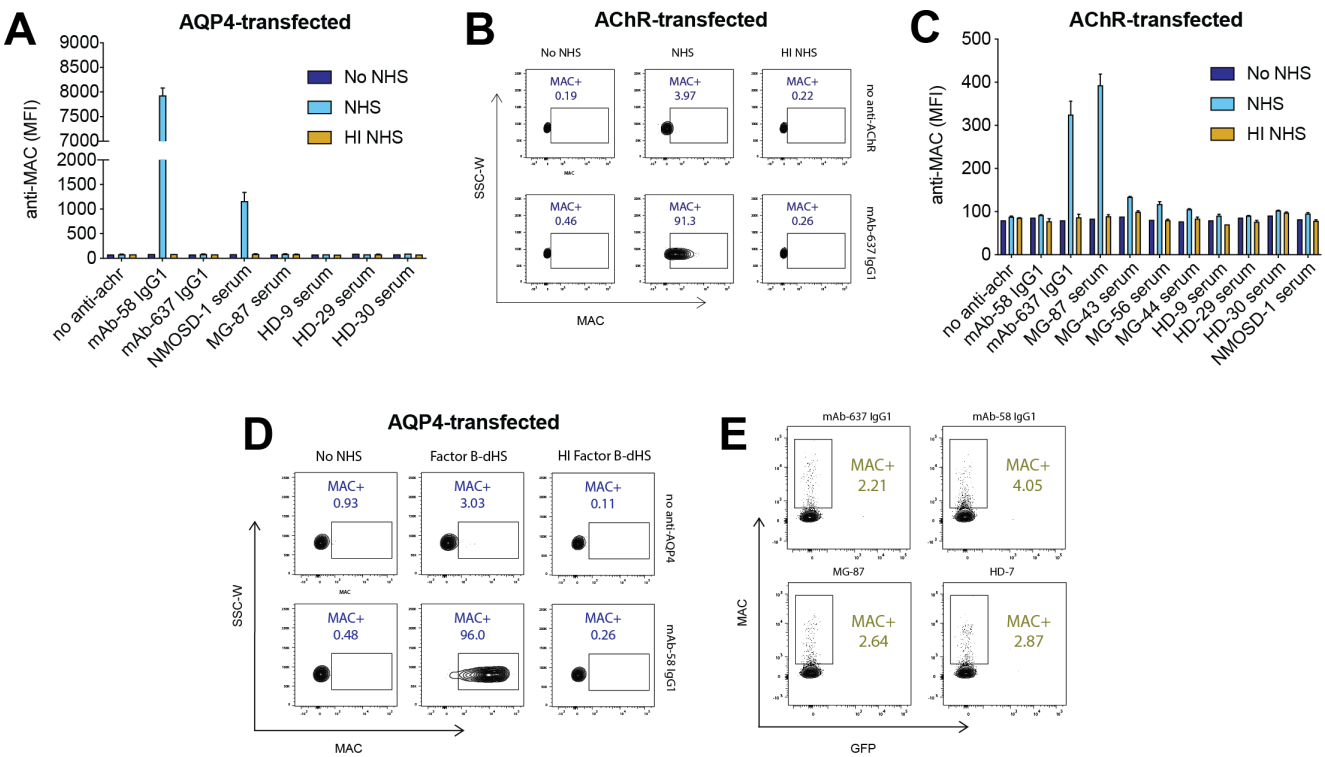

Figure 3. Autoantibody-mediated complement fixation assay with CD46/55/59 KO HEK293T cells. Autoantibodies were tested for their ability to mediate complement activation through measuring MAC formation on live cells, transfected with self-antigens, in which complement regulators were knocked out. **A.** Measurement of MAC deposition using an *in vitro* cell-based complement assay on AQP4 transfected CD46/55/59 KO HEK293T cells. Complement fixation was activated by the addition of NHS and anti-AQP4 antibody sources. Each bar represents the mean of duplicate experimental conditions. **B.** FACS analysis of AChR transfected CD46/55/59 KO HEK293T cells using an *in vitro* complement CBA. Very low MAC assemblies were detected using no complement source (normal human serum (NHS)), or heat inactivated normal human serum (HI NHS), while MAC-positive cells were observed when a monoclonal antibody (anti-AChR mAb-637 IgG1) was added with normal human serum. *Gating strategy:* CD46/55/59 KO HEK293T → single cell (SSC-W vs SSC-H) → single cells (FSC-W vs FSC-H) → AChR (GFP) positive cells. **C.** Measurement of MAC deposition using an *in vitro* complement CBA on AChR transfected CD46/55/59 KO HEK293T. Complement fixation was activated by the addition of NHS and anti-AChR antibody sources. No MAC deposition was observed with HD serum or non-binding antibodies. Each data bar represents the mean of duplicate experimental conditions. **D.** Factor B depleted NHS was used to test whether the alternative pathway contributed to autoantibody-mediated MAC deposition. AQP4 transfected cells were tested without (top row) or with the anti-AQP4 monoclonal mAb-58 IgG1 (bottom row). **E.** Un-transfected CD46/55/59 KO HEK293T cells were tested in the complement CBA using serum that included AChR autoantibodies or antigen-specific monoclonal antibodies, to test for non-specific MAC formation. Samples used in panels A-E: mAb-58 IgG1 (anti-AQP4 monoclonal), NMOSD patient (NMOSD-1), mAb-637 IgG1 (anti-AChR monoclonal), MG patient serum (MG-87, MG-43, MG-56, MG-44), and healthy donors (HD-9, HD-29, HD-30). Blank- no serum, NHS- normal human serum, HI NHS- heat inactivated normal human serum, Factor B-dHS- factor B depleted human serum, HI Factor B-dHS- heat inactivated factor B depleted human serum.

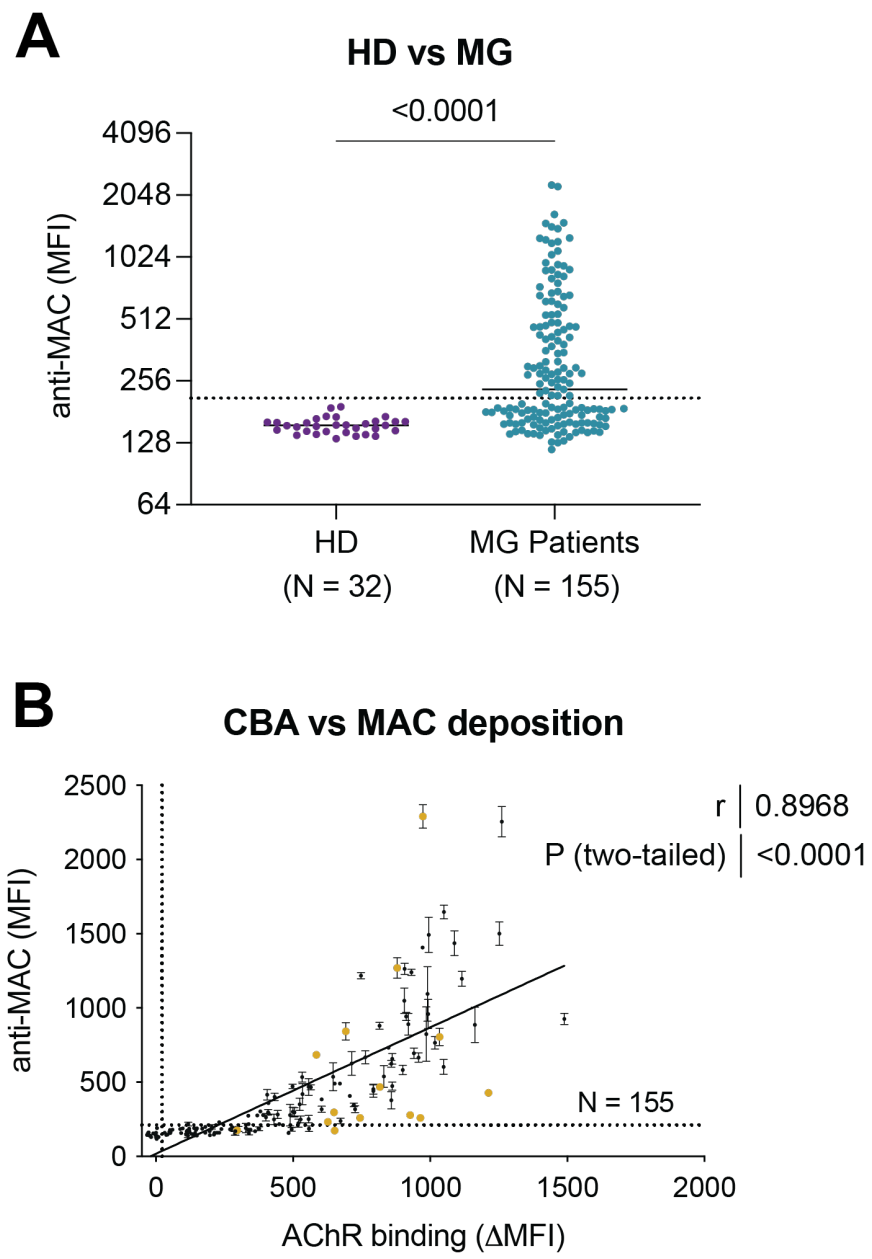

Figure 4. AChR autoantibody-mediated complement formation in MG patients. AChR autoantibodies in serum were tested for their ability to mediate complement activation through measuring MAC formation on live AChR-expressing CD46/55/59 KO HEK293T cells. **A.** Comparison of MAC deposition using serum samples (n=32) from HDs and serum samples (n=155) from AChR MG patients. The cutoff for positivity was set at the mean MFI + 4 STD (210.9 MFI) of the HD samples. Each data point represents the mean of triplicate experimental conditions. **B.** Correlation between MAC deposition and AChR autoantibody binding by CBA. Spearman correlation was used to calculate the relationship. The binding CBA cutoff for positivity was set at the mean MFI +4STD (21.91 ΔMFI) of the HD samples. Each data point represents the mean of triplicate experimental conditions. Colored (gold) points represent samples selected for further evaluation (*see Figure 5*).

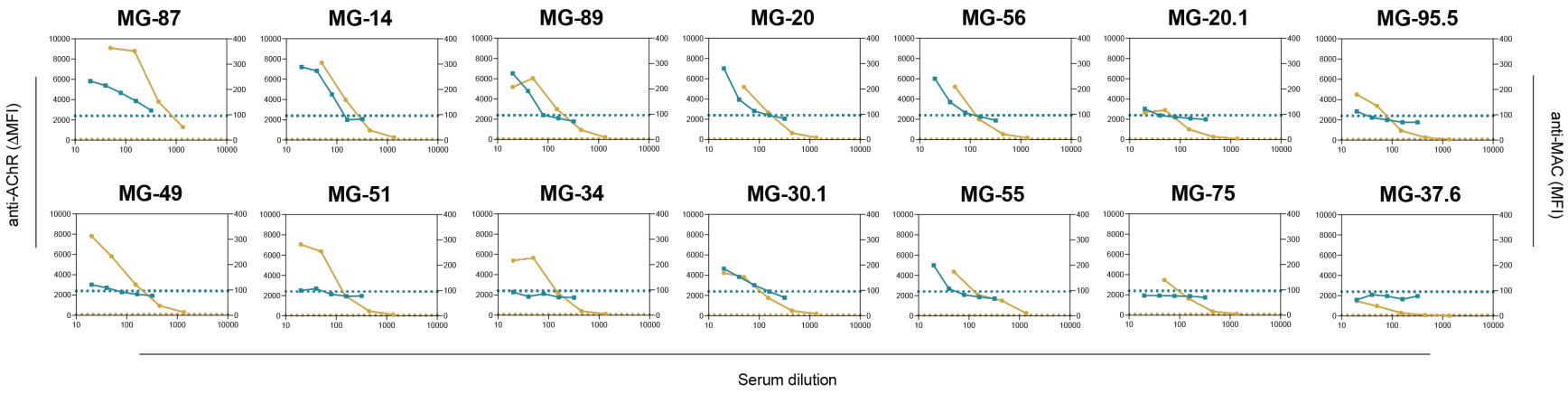

Figure 5: Heterogeneous AChR autoantibody-mediated complement formation. Samples screened in Figure 4B (indicated by golden points in Figure 4B) were examined side-by-side for both MAC formation and CBA binding. Each graph shows the data collected from individual serum samples. The x-axis represents the serum dilution of the sample tested for complement CBA (MAC) formation (blue dots) or CBA binding (golden dots). For AChR binding (left y-axis), samples were tested at serum dilutions of 1:20 plus 4 additional 3-fold dilutions (1:50, 1:150, 1:450 and 1:1350). For MAC formation (right y-axis), samples were tested at 2-fold serial dilutions (1:20, 1:40, 1:80, 1:160 and 1:320). Each data point represents the mean of experimental triplicate experimental conditions. Dotted horizonal lines mark the positive reactivity cut-off for complement (blue) and CBA binding (golden). Cutoffs were calculated using the mean MFI + 4STD of the HD samples (complement and CBA 96.01 MFI and 75.35 ΔMFI respectively).

Supplemental Figures and Tables

Heterogeneity of acetylcholine receptor autoantibody-mediated complement activity in patients with myasthenia gravis

eFigure 1. Representative flow cytometry plots of cell-based assay experiments with CHO cells.

eFigure 2. Representative flow cytometry plots of AChR autoantibody binding cell-based assay.

eTable 1. Demographics and clinical data of patient and control groups.

eTable 2. CRISPR gRNA sequences for the generation of CD46/55/59 KO HEK293T.

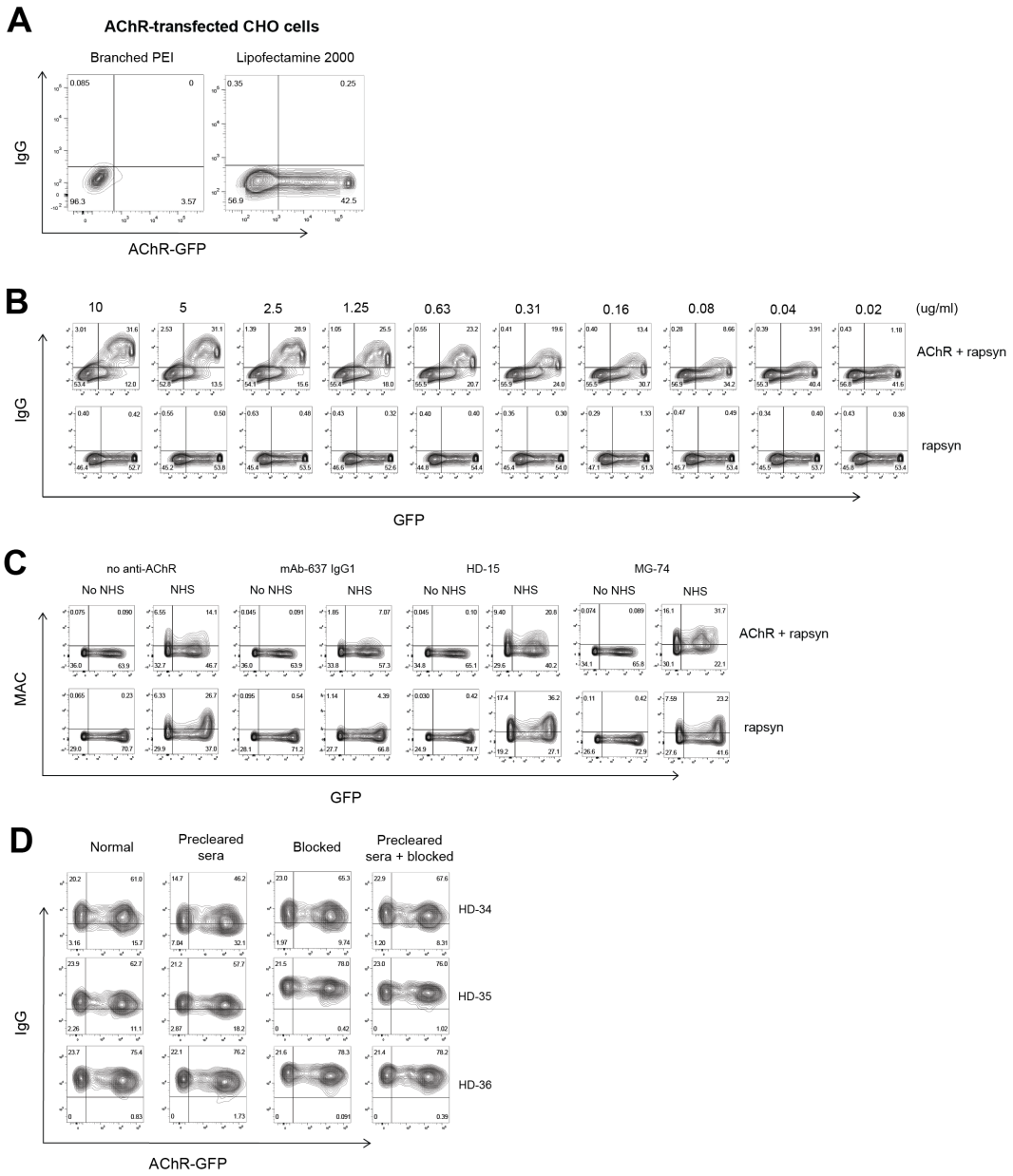

eFigure 1: Representative flow cytometry plots of cell-based assay experiments with CHO cells. A. Transfection of the AChR (co-transfected with Rapsyn) of CHO cells was tested with PEI and Lipofectamine 2000. Anti-human IgG was used for detection. **B.** Assessment of binding capacity of either AChR or rapsyn-only transfected CHO cells with the AChR-specific mAb-637 IgG1 over a broad range of concentrations (10 - 0.02 μg/ml). Anti-human IgG was used for detection. **C.** AChR-transfected CHO cells were tested for compatibility with the complement CBA protocol. NHS was used as complement source and either a HI HD serum, a HI MG serum or mAb-637 IgG1 were used as the autoantibody source. The legend indicates the conditions used for each presented plot. Anti-MAC was used for detection. **D.** CHO cells were transfected with rapsyn only. Different HI HD samples were added to the transfected cells that were either untreated or blocked with goat serum. The HI HD sera were either untreated or pre-cleared from CHO reactive cells by pre-incubation with CHO cells. Anti-IgG was used for detection.

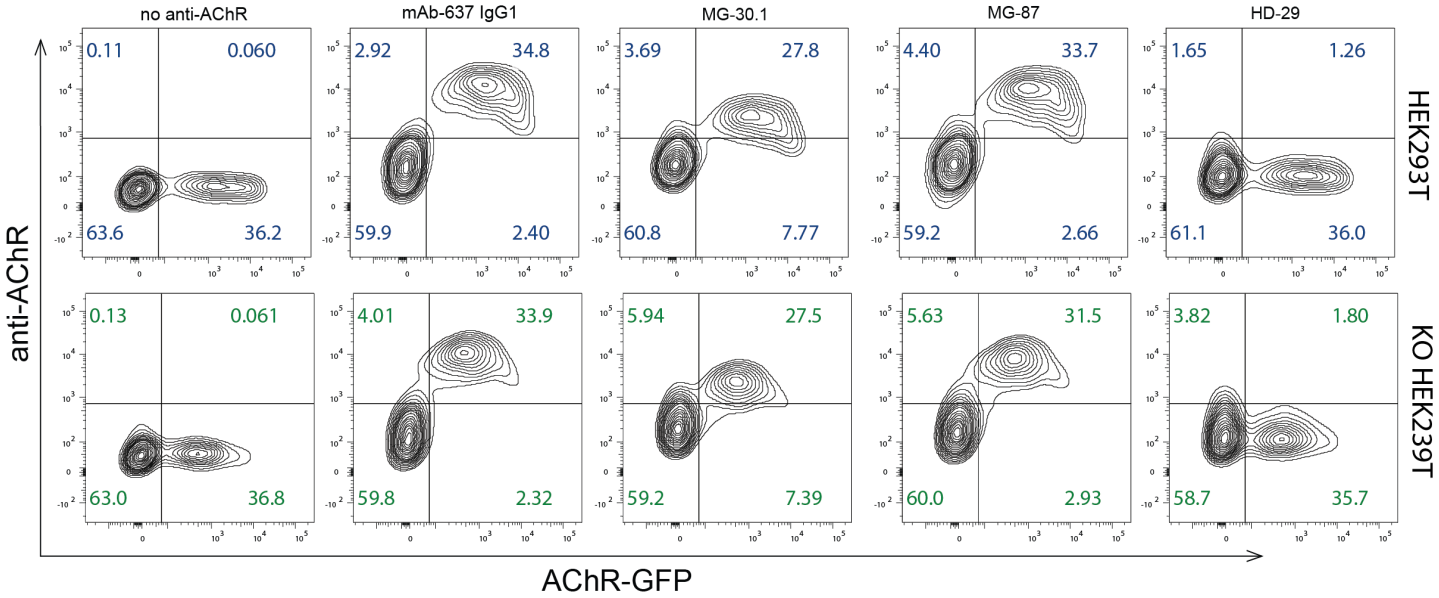

eFigure 2: Representative flow cytometry plots of AChR autoantibody binding. HEK293T or CD46/55/59 KO HEK293T cells transfected with AChR were tested with no anti-AChR, mAb-637 IgG1 (10ug/ml), MG patient serum (diluted 1:20), or HD serum (diluted 1:20). Binding was observed when cells were exposed to antibodies or patient serum. No difference in binding was observed between WT and KO cells.

eTable 1: Demographics and clinical data of patient and control groups.

Patient code[1]	Sex	Sample code[2]	Age[3]	EO vs LO[4]	MGFA class[5]	MGC[6]	AChR titer (nmol/L)[7]	anti-MAC (MFI)	AChR binding (ΔMFI)	Immuno therapy naïve[8]	Current Treatment[9]	Thymec-tomy[10]
1	F	1	90-100	LO	IIb	4	1.95	184.7	300.7	NO	Imuran, Prednisone, IVIg maintenance, mestinon	NO
2	M	2	90-100	LO	IIIb	17	13.7	536.0	646.3	NO	None	NO
3	F	3	90-100	LO	IIa	12	4.75	474.7	861.7	YES	Mestinon	NO
4	M	4	90-100	LO	I	4	9.07	439.7	793.0	YES	None	NO
5	M	5	80-89	LO	IIb	11	NA	347.7	721.7	NO	PLEX	NO
6	M	6	80-89	LO	I	3	0.3	141.7	-23.7	YES	None	NO
7	M	7	80-89	LO	I	4	2.22	264.3	400.7	YES	None	NO
8	M	8	80-89	LO	NA	NA	1.29	296.7	408.7	YES	None	NO
9	M	9	80-89	LO	V	42	66.5	657.3	861.3	NO	Prednisone	NO
10	M	10	80-89	LO	IIa	9	1.47	180.7	336.7	YES	None	NO
11	M	11	80-89	LO	I	NA	10.1	581.3	900.3	YES	None	NO
12	M	12	70-79	LO	I	NA	0.36	146.7	137.3	NO	Prednisone	NO
		12.1	70-79	LO	I	NA	NA	199.0	180.3	NO	Prednisone	NO
		12.2	70-79	LO	0	NA	0.46	189.7	139.3	NO	Prednisone	NO
13	M	13	70-79	LO	I	NA	0.22	156.7	52.0	YES	None	NO
14	F	14	70-79	LO	I	3	14.3	1269.0	879.7	YES	Mestinon	NO
15	F	15	70-79	LO	I	3	4.9	217.7	337.7	YES	None	NO
16	M	16	70-79	LO	IIIa	13	3.54	301.0	499.3	NO	Prednisone	YES
17	M	17	70-79	LO	I	7	0.55	187.7	150.0	NO	Prednisone	NO
		17.1	70-79	LO	I	2	0.55	147.3	42.7	NO	Imuran, Prednisone, Mestinon	NO
18	F	18	80-89	LO	IVb	18	25.3	453.7	793.0	YES	None	NO
19	F	19	70-79	LO	I	3	14.4	926.3	1489.7	YES	None	NO
20	F	20	70-79	LO	IVb	27	7.16	428.7	1212.7	YES	Mestinon	NO
		20.1	70-79	LO	IIb	5	1.23	259.0	964.0	NO	Prednisone, IVIg	NO
21	F	21	70-79	LO	I	4	23.2	157.7	339.0	NO	Prednisone, IVIg	NO
22	M	22	70-79	LO	IIb	3	1.38	160.3	180.3	NO	Prednisone, Pembrolizumab, IVIg	NO
		22.1	70-79	LO	IIA	7	9.51	156.7	816.0	NO	IVIg maintenance	NO
23	M	23	70-79	LO	0	0	0	118.7	3.3	NO	Prednisone, Azathioprine,	NO
24	F	24	70-79	LO	NA	0	1.29	170.7	361.3	NO	Prednisone, Methotrexate	NO
25	M	25	70-79	LO	IIIb	NA	4.85	534.3	532.7	YES	Mestinon	NO
26	M	26	70-79	LO	I	2	1.74	217.3	449.7	NO	Prednisone	NO
27	M	27	70-79	LO	I	7	7.8	491.3	651.7	YES	None	NO

28	M	28	70-79	LO	IIIb	11	12.8	186.7	376.0	NO	Prednisone, IVIg maintenance	NO
29	M	29	70-79	LO	0	0	0.02	186.7	169.0	NO	Prednisone	NO
30	M	30	70-79	LO	I	1	21.3	400.7	433.3	YES	Mestinon	NO
		30.1	70-79	LO	NA	8	92.3	842.3	692.0	YES	None	NO
31	M	31	60-69	LO	I	NA	4.15	359.0	410.0	YES	None	NO
		31.1	70-79	LO	I	4	24.7	695.7	940.7	NO	Imuran, Mestinon	NO
32	M	32	70-79	LO	0	0	5.88	251.3	557.3	YES	Imuran, Mestinon	NO
33	F	33	60-69	LO	I	NA	0.24	229.7	230.3	YES	None	NO
34	M	34	70-79	LO	IIb	3	1.82	232.3	627.3	NO	Prednisone	NO
35	M	35	60-69	LO	I	NA	35.2	880.3	815.7	YES	Mestinon	NO
36	F	36	70-79	LO	I	6	1.33	248.0	527.3	YES	Mestinon	NO
37	F	37	60-69	LO	IIIa	NA	11.7	420.0	534.7	NO	Prednisone, Mestinon, IVIg	YES
		37.1	60-69	LO	IIIa	NA	12.5	352.0	524.7	NO	Rituximab, Prednisone, mestinon	YES
		37.2	60-69	LO	IIIa	NA	12.2	296.0	505.3	NO	Mestinon, Prednisone	YES
		37.3	60-69	LO	IIa	5	3.51	278.0	390.7	NO	Prednisone	YES
		37.4	60-69	LO	0	0	2.19	197.7	277.7	NO	Prednisone, Mestinon	YES
		37.5	70-79	LO	I	3	5.46	178.7	275.0	NO	Prednisone	YES
		37.6	70-79	LO	IIIa	20	64.7	175.0	296.3	NO	Prednisone, Mestinon	YES
38	M	38	60-69	LO	IIIb	NA	10.3	302.7	380.3	YES	None	NO
39	M	39	60-69	LO	0	NA	0.92	147.3	211.3	NO	IVIg	NO
		39.1	60-69	LO	IVa	28	13.2	1436.0	1088.3	NO	Prednisone, PLEX	NO
40	M	40	60-69	LO	I	NA	0.95	141.7	149.3	NO	Imuran, Prednisone	NO
		40.1	60-69	LO	0	NA	0.47	141.3	141.0	NO	Rituximab, Imuran, Prednisone	NO
		40.2	60-69	LO	0	NA	0.4	146.3	109.9	NO	None	NO
41	M	41	60-69	LO	IIb	3	5.02	377.3	858.0	NO	None	NO
42	M	42	60-69	LO	0	0	0.99	179.0	51.3	NO	Rituximab, Prednisone	NO
		42.1	60-69	LO	0	NA	NA	185.0	88.3	NO	Rituximab, Prednisone	NO
		42.2	60-69	LO	0	0	0.77	180.3	60.7	NO	Rituximab, Prednisone	NO
		42.3	60-69	LO	0	0	0.46	159.0	32.0	NO	Prednisone	NO
		42.4	60-69	LO	0	0	0.2	165.7	53.3	NO	None	NO
		42.5	60-69	LO	0	0	0.51	165.0	49.3	NO	None	NO
		42.6	60-69	LO	0	NA	1.03	150.0	130.0	NO	None	NO
		42.7	60-69	LO	0	0	1.32	160.0	231.3	NO	None	NO

		42.8	60-69	LO	IIb	8	9.94	317.0	725.7	NO	None	NO
43	M	43	60-69	LO	I	7	14.3	182.7	495.0	YES	Mestinon	NO
44	M	44	60-69	LO	I	I	1.47	179.3	344.7	YES	None	NO
45	M	45	60-69	LO	V	NA	NA	318.3	604.7	NO	IVIg, IV solumedrol, PLEX	NO
46	F	46	60-69	LO	I	4	2.72	198.3	203.7	YES	Imuran, Mestinon	NO
47	M	47	60-69	LO	I	7	7.59	466.3	848.0	YES	None	NO
48	M	48	60-69	LO	I	3	49.2	1408.3	972.3	NO	Imuran, Prednisone	YES
49	M	49	60-69	LO	III	16	2.54	260.0	744.0	YES	None	NO
50	M	50	60-69	LO	IIb	3	8.08	160.0	214.0	NO	Prednisone, Mestinon	NO
51	M	51	60-69	LO	IVb	17	9.33	468.3	565.0	NO	Prednisone	NO
52	F	52	50-59	EO	0	NA	3.03	416.0	405.3	NO	Prednisone	YES
		52.1	50-59	EO	0	0	2.84	249.3	431.0	NO	None	YES
		52.2	60-69	EO	0	0	10.3	1647.3	1049.7	NO	None	YES
53	M	53	60-69	LO	I	5	0	139.3	-19.3	NO	Prednisone, Cellcept, IVIg maintenance	NO
54	F	54	60-69	LO	IIb	6	147	623.7	858.7	YES	None	NO
55	M	55	60-69	LO	0	4	11.4	684.0	585.3	NO	IVIg maintenance	YES
56	M	56	60-69	LO	IVb	28	88	277.7	927.7	YES	Mestinon	NO
57	F	57	60-69	LO	IIb	13	1.17	145.3	-1.3	NO	Prednisone, Mestinon, IVIg	NO
58	F	58	50-59	EO	IIb	NA	NA	1217.7	748.2	NO	Imuran, Prednisone	YES
59	M	59	50-59	LO	I	7	3.17	186.3	203.0	YES	None	NO
		59.1	50-59	LO	0	0	8.2	170.7	289.3	NO	Prednisone, IVIg maintenance	NO
60	F	60	50-59	LO	I	4	NA	170.0	196.0	NO	Prednisone, Mestinon, Cellcept	YES
61	M	61	50-59	LO	0	0	0	158.0	92.3	NO	Prednisone, Mestinon	NO
	M	61.1	50-59	LO	I	8	NA	189.0	373.7	NO	None	NO
62	F	62	50-59	EO	NA	NA	44.8	2254.3	1261.3	NO	Mestinon	YES
		62.1	50-59	EO	IIIb	NA	3.31	279.0	489.3	NO	Imuran, Prednisone, IVIGg	YES
63	F	63	50-59	EO	IIa	NA	123	1500.3	1252.7	YES	Mestinon	NO
64	M	64	50-59	LO	IIIb	0	13.5	889.7	920.7	YES	None	YES
65	M	65	50-59	LO	IVb	23	35.7	886.7	1162.7	NO	Prednisone, Mestinon	NO
		65.1	50-59	LO	IIb	10	15.2	602.7	1048.7	NO	Prednisone, Mestinon, IVIGg	NO

		65.2	50-59	LO	0	0	15.8	468.3	557.2	NO	Prednisone, Mestinon	NO
66	M	66	50-59	LO	IIIb	10	9.7	223.0	519.3	NO	Prednisone, Mestinon	NO
67	F	67	50-59	LO	IIa	2	4.9	490.7	671.3	NO	Prednisone, Mestinon, Cellcept	NO
68	M	68	50-59	LO	I	3	100	143.7	197.0	YES	None	NO
69	F	69	40-49	EO	I	2	2.7	764.7	1017.0	NO	Methotrexate	NO
70	F	70	50-59	EO	IIb	12	16.6	733.0	652.0	NO	Cellcept, Mestinon, IVIg maintenance	YES
71	M	71	40-49	EO	IIa	9	0	157.7	-28.3	YES	None	NO
72	F	72	40-49	EO	IIIb	17	11.5	824.7	986.3	NO	Prednisone, Cellcept, Mestinon	YES
		72.1	40-49	EO	0	0	7.29	625.0	713.3	NO	Prednisone, Cellcept, IVIg maintenance	YES
73	F	73	40-49	EO	0	NA	5.05	190.3	327.3	NO	Imuran	YES
		73.1	40-49	EO	IIb	2	16.8	183.0	270.7	NO	None	YES
74	F	74	40-49	EO	IIIa	19	NA	665.3	957.3	NO	None	YES
75	F	75	40-49	EO	IIB	10	11.3	174.3	483.3	NO	Prednisone, Imuran, IVIg maintenance, Mestinon	YES
76	F	76	30-39	EO	0	0	3.73	408.3	707.0	NO	Imuran	YES
77	F	77	30-39	EO	0	NA	0.27	128.3	0.0	NO	IVIg maintenance	YES
78	F	78	40-49	EO	IIIb	19	22.2	1095.0	990.3	NO	Cellcept	YES
79	F	79	30-39	EO	IIIb	13	39	1493.3	994.7	NO	Prednisone, IVIg	YES
		79.1	40-49	EO	IIIb	7	22.8	1196.3	1115.7	NO	Prednisone, Mestinon, Cellcept, IVIg	YES
80	F	80	30-39	EO	I	NA	NA	129.3	10.0	NO	Prednisone	NO
		80.1	30-39	EO	I	5	0	160.0	0.0	NO	Prednisone	NO
81	F	81	30-39	EO	0	0	20	137.0	3.6	NO	Mestinon, IVIg	NO
		81.1	30-39	EO	IIa	7	8.14	131.0	-18.0	NO	Mestinon, IVIg	YES
82	F	82	30-39	EO	I	5	0.41	154.3	-9.4	YES	Mestinon	NO
		82.1	30-39	EO	IIb	11	0.22	161.0	-26.7	NO	Prednisone, Mestinon	NO
		82.2	30-39	EO	IIb	8	0.25	145.0	-32.0	NO	Prednisone, IVIg maintenance	YES
		82.3	30-39	EO	IIb	6	0.25	144.0	-31.0	NO	Prednisone, IVIg maintenance	YES
83	F	83	30-39	EO	IIIb	NA	0.61	472.7	498.3	NO	Mestinon	YES
84	F	84	30-39	EO	0	NA	4.15	282.7	444.0	NO	Prednisone	YES

		84.1	30-39	EO	IIa	3	9.19	667.7	763.3	NO	Prednisone	YES
		84.2	30-39	EO	0	0	0.82	177.7	145.7	NO	Rituximab, Prednisone	YES
		84.3	30-39	EO	0	0	0.48	189.3	97.7	NO	Rituximab, Prednisone	YES
		84.4	30-39	EO	0	NA	0.64	185.7	121.8	NO	Rituximab, Prednisone	YES
		84.5	30-39	EO	0	0	0.72	167.0	112.7	NO	Prednisone	YES
		84.6	30-39	EO	0	0	0.73	168.3	122.0	NO	Prednisone	YES
		84.7	30-39	EO	0	0	0.97	174.0	114.3	NO	Prednisone	YES
		84.8	30-39	EO	0	0	2.37	186.0	148.0	NO	Prednisone	YES
		84.9	30-39	EO	0	0	3.28	217.3	118.3	NO	None	YES
		84.10	30-39	EO	0	0	2.79	184.7	238.3	NO	None	YES
85	M	85	30-39	EO	I	0	0	190.3	4.0	YES	Mestinon	NO
		85.1	30-39	EO	I	1	0	151.3	-3.0	NO	Prednisone, Mestinon	NO
86	M	86	30-39	EO	0	2	0.01	158.0	142.7	NO	Imuran	YES
87	F	87	30-39	EO	IIa	5	43.1	806.0	1034.7	NO	Prednisone, Mestinon	YES
88	M	88	30-39	EO	IIIa	15	27.4	1241.0	931.7	YES	None	NO
		88.1	30-39	EO	IIb	8	45.5	1263.0	906.7	NO	Prednisone	NO
89	F	89	30-39	EO	IIa	NA	89.8	2290.0	973.5	NO	Mestinon	YES
90	F	90	30-39	EO	IIa	2	NA	942.0	912.3	NO	Mestinon, IVIg maintenance	YES
91	F	91	30-39	EO	Ivb	31	2.47	239.0	673.3	NO	Rituximab, Mestinon, IVIg maintenance	YES
		91.1	30-39	EO	IIIb	28	0.83	187.3	558.3	NO	Rituximab, IVIg maintenance	YES
92	F	92	20-29	EO	0	NA	6.61	274.3	336.7	NO	None	YES
93	M	93	20-29	EO	IVb	20	10.1	960.0	993.0	NO	Prednisone, Azathioprine,	NO
94	F	94	20-29	EO	IIIb	12	0.68	160.0	223.4	NO	Mestinon	YES
		94.1	20-29	EO	I	1	0.49	155.3	288.0	NO	Prednisone, IVIg	YES
95	M	95	10-19	EO	IIa	4	12	1049.3	905.3	NO	Prednisone, IVIg maintenance	YES
		95.1	10-19	EO	IIa	0	12	539.3	830.7	NO	Rituximab, Prednisone, IVIg maintenance	YES
		95.2	10-19	EO	IIa	4	6.66	384.7	604.7	NO	Rituximab, Prednisone, IVIg maintenance	YES
		95.3	10-19	EO	IIa	1	8.89	289.0	411.7	NO	Rituximab, Prednisone, IVIg maintenance	YES

		95.4	10-19	EO	0	0	5.75	275.7	369.7	NO	Mestinon	YES
		95.5	10-19	EO	0	0	10	296.0	649.0	NO	None	YES
96	M	96	10-19	EO	0	0	0.1	140.0	117.3	NO	Prednisone, Mestinon	YES
97	M	97	60-69	LO	I	1	0.46	144.3	37.7	YES	None	NO

Healthy donors (HD)

HD code[1]	Sex	Sample code[2]	Age[3]
1	F	1	20-29
2	F	2	30-39
3	M	3	30-39
4	M	4	30-39
5	M	5	40-49
6	M	6	20-29
7	F	7	20-29
8	M	8	20-29
9	F	9	20-29
10	F	10	60-69
11	M	11	60-69
12	M	12	30-39
13	F	13	30-39
14	M	14	30-39
15	M	15	20-29
16	M	16	20-29
17	F	17	50-59
18	M	18	40-49
19	M	19	30-39
20	M	20	30-39
21	M	21	30-39
22	M	22	20-29
23	F	23	30-39
24	M	24	20-29
25	F	25	20-29
26	M	26	20-29
27	F	27	20-29
28	F	28	20-29
29	M	29	20-29
		29.1	20-29
30	F	30	20-29
		30.1	20-29
31	F	31	50-59
32	M	32	30-39
33	F	33	20-29
34	M	34	50-59

35	F	35	20-29			
36	M	36	30-39			
Neuromyelitis optica spectrum disorder (NMOSD)						
Patient code[1]	**Sex**	**Sample code[2]**	**Age[3]**	**Autoantibody status**	**Immunotherapy naïve[8]**	
1	F	1	60-69	AQP4+	YES	

Abbreviations: M = Male; F = Female; NA = Not available, EO = Early-onset MG; LO = Late-onset MG

[1, 2] Each patient code consists of either one or multiple longitudinal serum samples. Longitudinal samples are listed in chronological order.

[3] Patient age range (years) at time of sample collection.

[4] Early onset vs late onset MG was determined by age of diagnosis: early-onset (<50 years); late-onset MG (≥50 years).

[5] The MGFA Clinical Classification.

[6] The MG composite (MGC) score.

[7] Serum sample AChR titer (nmol/L) as measured by RIA.

[8] Immunotherapy includes cellcept, prednisone, azathioprine, methotrexate, IV solumedrol, IV immunoglobulin, rituximab and PLEX.

[9] Treatment at time of sample collection. Rituximab treatment is reported if it is within 6 months of sample collection. IVIg and PLEX treatment reported if administered within 12 weeks of sample collection. IVIg maintenance or PLEX maintenance is reported if treatment administration is recurring.

[10] Thymectomy status at time of sample collection.

eTable 2: CRISPR gRNA sequences for the generation of CD46/55/59 KO HEK293T

Gene	NCBI gene ID	Primer Name	gRNA sequence (5'-3')
hCD46	4179	Anti	TCTAGACAGGGGGTCACCGT
		Sense	AAAGTATGAAGACCATGTAG
hCD55	1604	Sense	(G)AAATGACTCCCACCCGAACA
		Sense	(G)AGAAAATAGTGTCAATCAGA
hCD59	966	Anti	GTGGCAGTGCCTGTAAACCA
		Sense	GCTGAGCTCAAAGGACACGT